2016

Numerical Simulation (CFD) to Explore Optimal Vortex Generator Array Configurations in Air Cooled Condensers

Mei Yung Wong
University of Illinois at Urbana Champaign, United States of America, mwong17@illinois.edu

Gregory D Hardy
University of Illinois at Urbana Champaign, United States of America, ghardy2@illinois.edu

Anthony M Jacobi
University of Illinois at Urbana Champaign, United States of America, a-jacobi@illinois.edu

Predrag Hrnjak
University of Illinois at Urbana Champaign, United States of America, pega@illinois.edu

Numerical Simulation (CFD) to Explore Optimal Vortex Generator Array Configurations in Air Cooled Condensers

Mei Yung WONG[1], Gregory D. HARDY[1], Anthony M. JACOBI[1]*, Predrag HRNJAK[1]

[1]University of Illinois at Urbana Champaign, Mechanical Science and Engineering, Urbana, IL, USA

* Corresponding Author
(Phone-(217) 333-4108, Fax-(217) 244-6534, E-mail-a-jacobi@illinois.edu)

ABSTRACT

This study presents a numerical analysis of laminar convective heat transfer in a rectangular channel with an array of delta-winglet vortex generators (VG) and with one straight line of multiple VGs. A low and high Reynolds number case of 225 and 1123 is simulated which is representative of the lower and upper limits of the air velocity range in a typical air cooled condenser (ACC) system. The effects of interacting and non-interacting vortices on the Nusselt number and pressure drop are observed for the two Reynolds numbers. The low Re cases flow cleaner through the channel, pressure drop is slightly lower for the array in comparison to the straight line formation for two VG pairs, however the increase in Nusselt number is higher in the straight line configuration. For the high Re cases the vortices generated are stronger and persist longer and interactions between vortices in the array configuration lead to Nusselt number increase but a higher pressure drop increase. The straight line configuration has almost equal increase in Nusselt number and pressure drop.

1. INTRODUCTION

Heat exchangers such as evaporators and condensers are a major component in applications of air conditioning, refrigeration and power conversion systems. ACC used in power stations reject heat to the environment very similarly to air conditioning systems. Rejection of heat to the ambient air is not very efficient and a more effective design is sought in the fin component of the condenser. Passive flow manipulation techniques are implemented by placing vortex generators on the heat transfer surface to create vorticity parallel to the main flow. Several researchers have studied the implementation of different geometries of VGs both numerically and experimentally in different heat exchanger applications. Research on this technique has shown that the heat transfer enhancement exceeds the pressure drop penalty, thus having promising potential.

It is anticipated that creating arrays of delta-winglets will generate further enhancement of heat transfer if constructive interference between vortices occurs, while not increasing the pressure drop significantly. Two challenges arise in designing such systems. The winglets must be spaced far apart to avoid destructive interference but close enough to enhance as much surface area as possible. The generated vortex must also be able to flow cleanly through the passage. First, flow visualization experiments were performed in a water tunnel to guide the design and placement of delta winglets. Based on the conclusions from these experiments, a numerical simulation of VG array configurations is performed to study the heat transfer and pressure drop characteristics compared to a baseline case with no VGs.

2. LITERATURE REVIEW

Leu *et al.* (2004) performed numerical and experimental analyses to study heat transfer and flow in the plate-fin and tube heat exchangers with inclined block shaped VGs mounted behind the tubes. Different span angles and Reynolds numbers ranging from 400 to 3000 were investigated. The best improvement was seen in the case of a 45° angle with a fin area reduction of 25% at Re_{Dh} = 500. Joarder and Jacobi (2007) numerically studied a seven-row inline tube heat exchanger with various arrangements of delta winglet arrays. The Reynolds number ranged from 330 to 850. They found that the impingement of winglet redirected flow on the downstream tube is an important mechanism for heat transfer augmentation. At Re=850, the 3VG inline array achieved a 74% enhancement in j factor over the base case and an associated pressure drop increase of 41%. Wu and Tao (2008a, 2008b) numerically

studied laminar heat transfer in a rectangular channel with a pair of punched rectangular VGs. They studied the effects of the thickness of the VG and the punched holes to heat transfer and flow characteristics. In their studies, they found that the case with punched VG holes had a better heat transfer enhancement near the VG and a lower average friction factor compared to the case without the punched holes. In part B of their studies, they concluded that a delta winglet pair is more effective on the heat transfer enhancement than a rectangular winglet pair. Tian *et al.* (2009) performed three dimensional numerical simulations comparing two different shapes (rectangular and delta winglet pair) and configurations (common flow-up and common flow-down) of a VG pair on a flat plate channel. The delta winglet pair performed better while the two different configurations had the same overall performance. They observed an increase in the Nusselt number by 8-46% with pressure drop increase of 20-64% in the rectangular winglet pair and 3-26% with a pressure drop increase of 7-22% in the delta winglet pair. He *et al.* (2013) numerically investigated the heat transfer enhancement and pressure loss for fin and tube heat exchangers with rectangular winglet pairs placed in an in-line and staggered arrangement. They determined that a staggered arrangement of the winglet pairs led to a reduction in the pressure drop penalty by 4.5-8.3% without any loss in heat transfer enhancement. They conclude that the phenomenon can be attributed to the asymmetric distributions of temperature field and pressure gradient. Dezan *et al.* (2015) studied the interaction effects between parameters for a flat-tube louvered fin heat exchanger using delta-winglets. The input parameters were louver angle, angle of attack and stream wise position of the delta winglet. The Reynolds numbers used were 120 and 240 based on hydraulic diameter. They found that the louver angle was the main contributor to friction factor regardless of the Reynolds numbers. The contribution of each parameter to heat transfer is strongly associated with the type of geometry and Reynolds numbers. For lower Reynolds number, the major contributor is the louver angle and for higher Reynolds numbers, the parameters of the delta winglet pair is the major contributor in particular their angle of attack.

Fiebig *et al.* (1993) experimentally studied the effect of delta winglet vortex generators on heat transfer and pressure drop of a fin and tube heat exchanger element. Four configurations were tested in an inline and staggered arrangement for Reynolds number ranging from 600 – 2700. They measured a 55-65% heat transfer enhancement for the inline tube arrangement with a 20-45% increase in the apparent friction factor. The corresponding increases were lower for the staggered arrangement. Fiebig *et al.* (1994) studied heat transfer and flow loss in fin tube with flat and round tubes. They found that implementing wing type vortex generators increase heat transfer marginally about 10% for round tubes but dramatically, about 100% for the flat tubes. The heat exchanger element with flat tubes had nearly twice as much heat transfer and half as much pressure loss as the heat exchanger element with round tubes. Wang *et al.* (2002) studied the local and average heat/mass transfer characteristics over a flat tube bank fin with four vortex generators per tube. The mass transfer experiments are performed using naphthalene sublimation method and an analogy between heat and mass transfer is used to obtain the local and average heat transfer characteristics. Heat transfer enhancements reached 47.5%, 41.4% and 37.5% with identical mass flow rate, pumping power and pressure drop constraints when compared with flat tube fin element without VG.

A full scale prototype heat exchanger with VGs was tested by Elsherbini and Jacobi (2002) with leading edge delta-wing type VG for plain fin and tube heat exchanger applications. Heat transfer enhancements up to 31% was obtained with no significant pressure drop increase. Joarder and Jacobi (2005) performed full scale wind tunnel testing of a compact heat exchanger for automotive applications with delta-wing type VG. An average heat transfer enhancement of 21-23.4% was seen in dry and wet conditions over the baseline with an increase in pressure drop of less than 7%. The authors (2008) also performed full scale testing of compact plain fin and tube heat exchanger. Reynolds number range of 220 to 960 was studied. It was found that the heat transfer coefficient increases from 16.5% to 44% for a single row winglet arrangement with a pressure drop increase of less than 12%. For a three row VG array placed in alternate tubes, the enhancement in heat transfer increases from 19.9% to 68.8% with increased pressure drop penalty from 87.5% to 26%.

The results from various studies indicate that VGs have a potential to reduce the area of heat transfer and size of the heat exchangers considerably for a given heat load.

3. RESEARCH METHODS

3.1 Flow Visualization and Mass Transfer Experiments

3.1.1 Dye-in-water flow visualization experiments were conducted in a closed-circuit water tunnel. These tests

allowed for quick screening of many VG array configurations. The water tunnel reservoirs and tunnel contraction were constructed from reinforced fiberglass. A honeycomb screen was inserted upstream of the tunnel contraction and test section to orient the flow. Water flow was driven by a 0.37 kW, 230 V, single phase, AC induction motor. Velocity was measured by recording the time required for a drop of dye to traverse the test section. The test section was made from clear cast acrylic and measured 18 in. x 12 in. x 12 in. A parallel flow channel was created by mounting two 12 in. x 12 in. x 3/32 in. sheets of clear acrylic in the test section. The bottom channel sheet was fixed about two inches above the bottom test section wall. The top channel sheet was installed in such a way to allow the experimenter to change the channel spacing by indexing the top sheet vertically. A mirror was mounted at an angle beneath the test section to give clear view of the flow and allow video capture from a camera and tripod set-up. The dye injection system consisted of three separate 250 mL dye reservoirs. Food coloring dye was used as a tracer. The dye was gravity fed into the test channel using 0.5 mm microinjection tubes bent in the flow direction. The volume flow rate of each dye stream was regulated by a needle valve in the dye supply tubing. The effect of VGs in an array is seen in Figure 1.

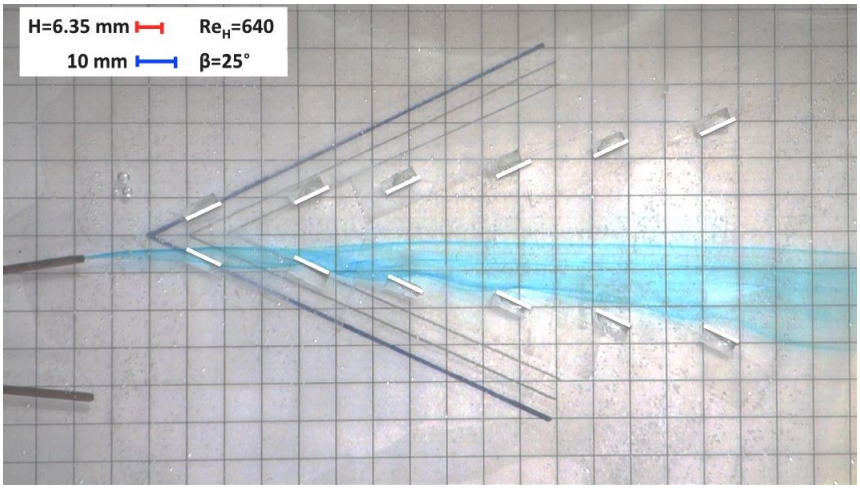

Figure 1: Flow visualization in water tunnel

3.1.2 An open-circuit wind tunnel was used to conduct naphthalene sublimation mass transfer experiments. The wind tunnel outlet was directed to another room and out a window to ensure that the air entering the wind tunnel would not be contaminated with naphthalene. A honeycomb screen was installed at the tunnel inlet to orient the flow. The flow was passed through a 9:1 contraction to create a flat velocity profile. The test section was made from 0.5 in. thick, clear acrylic. The interior cross section of the test section was 6 in. x 6 in. At the front of the test section, 0.1 in. wide and 0.125 in. deep grooves were cut into the sidewalls to house fifteen fins. The grooves were cut to the same length to minimize the growth of the velocity boundary layers. Thirteen fins were made from acrylic and two from aluminum, all measuring 250 mm x146 mm x 2.38 mm. This formed sixteen rectangular channels. Two 12 mm holes (one in the sidewall and one in the bottom wall) were drilled in the test section downstream of the fins. This was done so that a hotwire anemometer could be inserted to calibrate the pump speed versus air velocity prior to testing. The holes were covered with airtight plugs during sublimation experiments. A 60 mm x 200 mm x 1 mm cavity was milled out of each aluminum fin to house the naphthalene sample. The cavity starts 0.5 mm from the leading edge of the fin in order to protect the naphthalene sample from excessive sublimation and flow-altering shape deformation. This small offset from the leading edge causes an unheated starting length, however the effect was determined to be negligible.

The naphthalene sublimation technique utilizes mass transfer in convective flow in order to determine heat transfer coefficients. The technique used in these experiments is an established method and is well explained by Mendes (1991). Naphthalene is used because it sublimes readily under ambient conditions. A major advantage is that the technique simulates adiabatic and isothermal boundary conditions without introducing errors due to conduction and radiation heat transfer. Scintillation grade (+99% pure) naphthalene was casted into each fin cavity. The naphthalene was heated using a hot water bath. First a large beaker of water is heated on a hot plate above the melting point of naphthalene. Then another beaker containing naphthalene is submerged in the water bath until the water level is higher than that of the naphthalene and it is allowed to melt. The cavity in the aluminum fin is lined with aluminum tape to create a barrier and preheated using a second hot plate. The barrier is used to contain the naphthalene when

overfilling the cavity and preheating prevents the molten naphthalene from solidifying too quickly. Naphthalene solidifies irregularly so it must be sanded down to produce a smooth and uniform surface. First, 60 grit sandpaper was used to quickly remove large irregularities and then 120 grit sand paper is used to smooth the remaining material. The sand paper was wrapped around a small wooden block larger than the width of the cavity to ensure a level surface. Finally, the fin sample was sanded around the cavity and cleaned using isopropyl alcohol in order to remove solidified naphthalene and dust. Care was taken to minimize the amount of time between completion of naphthalene casting and installation of the sample in the wind tunnel.

Before each test (and before casting) a template of the VG array was printed and cut out and double sided was adhered to each VG. The template was used to mark the position and attack angle of each VG in the array on the sample. This allowed the VGs to be placed and the fins weighed and installed in as little as five minutes after exposing the sample to ambient air. The samples were measured using a mass balance with a ±0.005 gram error. The naphthalene fins were installed in the center of the test section cross-section and exposed to airflow at varying velocities. Air temperature at the wind tunnel inlet was recorded in 30-second intervals using a data logger for the duration of the experiment. The temperature was monitored to ensure there were no fluctuations beyond ±0.5 ºC. Due to the sensitivity of naphthalene vapor pressure to air temperature, changes greater than 1 ºC causes significant error in measured mass transfer coefficients. Preliminary tests were run to determine the optimal test duration. For all cases, duration of 2-3 hours was sufficient to sublime a measurable amount of naphthalene while minimizing changes in the cast geometry. After each test, the samples were weighed and recorded immediately. A small experiment was performed to account for any sublimation due to natural convection during sample preparation. Each sample was allowed to sublime under ambient conditions for four minutes. The change in mass was recorded using a precision mass balance with ±0.00005 uncertainty. The mass change due to natural sublimation was negligible in comparison to the smallest mass change during testing. The data was reduced to calculate Reynolds number, average mass transfer coefficient, and average Sherwood Number, and the average Nusselt number was determined using the heat and mass transfer analogy.

$$\bar{h}_m = \frac{\Delta m}{A_n \rho_{n,v} \Delta t} \tag{1}$$

$$\overline{Sh} = \frac{\bar{h}_m D_h}{D_{n,a}} \tag{2}$$

$$\overline{Nu} = \overline{Sh}\left(\frac{\mathrm{Pr}}{Sc}\right)^{0.34} \tag{3}$$

3.2 Numerical Simulation

3.2.1 Governing equations: The equations used are the Navier-Stokes continuity, momentum and energy equations as described in equations 4-6. The fluid is assumed to be incompressible with constant properties, negligible viscous dissipation and buoyancy effects. The flow is laminar, steady and three dimensional.

$$\frac{\partial}{\partial x_i}(\rho u_i) = 0 \tag{4}$$

$$\frac{\partial}{\partial x_i}(\rho u_i u_j) = -\frac{\partial P}{\partial x_j} + \frac{\partial}{\partial x_i}(\mu \frac{\partial u_j}{\partial x_i}) \tag{5}$$

$$\frac{\partial}{\partial x_i}(\rho u_i T) = \frac{\partial}{\partial x_i}\left(\frac{k}{c_p}\frac{\partial T}{\partial x_i}\right) \tag{6}$$

3.2.2 Boundary conditions: A plain channel represents one single element in a plain-fin flat tube cross flow heat exchanger and is used as the fin model. All flow variables are initialized at zero except for a prescribed inlet velocity, inlet temperature and constant wall temperatures. The flow is simulated in half the duct as the placement of

VG pairs is symmetric. A uniform wall temperature is prescribed at three walls with a no slip boundary condition and a symmetry condition is prescribed on the fourth side along the axis of symmetry. The computational domain is extended downstream such that a fully developed outflow boundary condition is prescribed at the outlet. In the case where VGs were present, a no slip boundary condition was used with a constant temperature of the wall. The geometry of the fin being simulated is shown in Figure2. The actual fin dimensions are 19x2x200 mm (BxHxL).

- Inlet(z=0) : $u = u_\infty; v = w = 0; T = T_\infty$ (7a)
- Outlet(z=L) : $\frac{\partial u}{\partial z} = \frac{\partial v}{\partial z} = \frac{\partial w}{\partial z} = 0, \frac{\partial T}{\partial z} = 0$ (7b)
- Symmetric plane (x=0) : $u = 0; \frac{\partial v}{\partial x} = \frac{\partial w}{\partial x} = 0; \frac{\partial T}{\partial x} = 0$ (7c)
- Side walls (x=B/2, y=0, y=H) : $u = v = w = 0; T = T_w$ (7d)

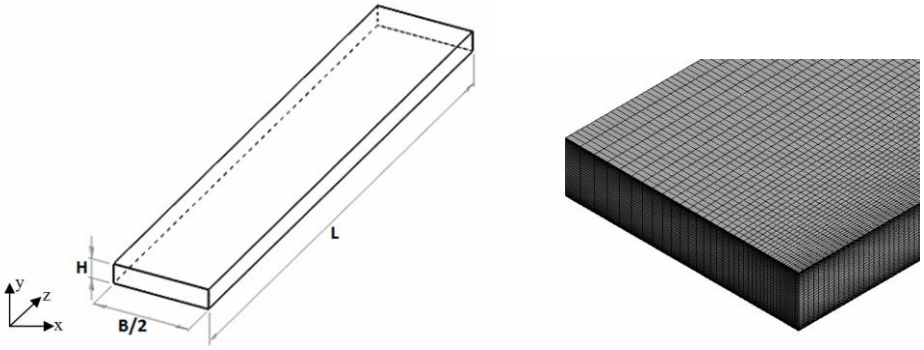

Figure2: Computational domain and mesh

3.2.3 Geometry: The VGs used are delta winglets with dimensions of 2x3 mm and thickness 0.25mm. The VG are placed at an angle of attack of 30°. The array is placed in a V-shaped configuration where the tip of the downstream VG is in line with the tail end of the preceding VG. The first VG pair is separated by a distance of 2mm from each other. The second and third pairs are placed two cord lengths distance downstream of the flow. The straight line configuration has two pairs of VGs placed in the same xy-plane, at a distance such that there is no interaction of the vortices. Only a quarter of the full length (L) is studied for effective area of enhancement with the idea that the placement of the VG rows will be repeated in the sections downstream of the flow. The geometry of a 3VG row and a straight line configuration are shown in Figure 3. The intermediate mesh as described in the grid independence section is used with a finer distribution of cells around the VG.

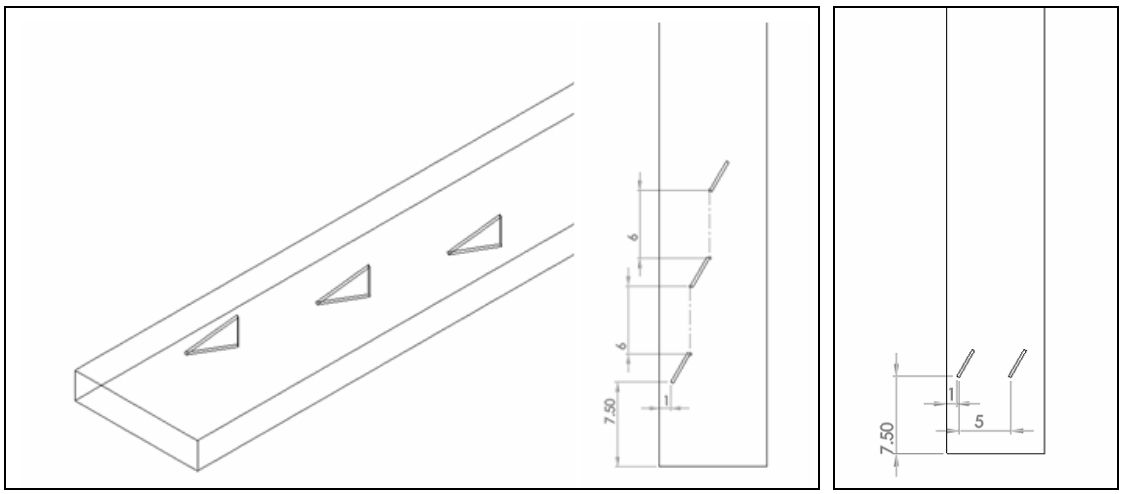

Figure 3: Isometric and top view of the 3VG pair array, top view of straight line configuration

3.2.4 Numerical method: A commercial finite volume based CFD software, ANSYS Fluent is used for solving the governing equations with the prescribed boundary conditions. A Semi-Implicit Method for Pressure Linked Equations-Consistent (SIMPLEC) was used for the coupling and correction of pressure and velocity terms. The second order upwind scheme is used for the momentum and energy terms and a second order accuracy is obtained in the pressure term. Scaled residuals of continuity and momentum equations are set to 10^{-5} and energy equations are converged to 10^{-8}.

Nusselt number (Nu) is defined by the equation:

$$Nu = \frac{hL}{k} \tag{8}$$

Where the h is the surface heat transfer coefficient is given by the equation:

$$h = \frac{q}{T_w - T_m} \tag{9}$$

4. NUMERICAL VALIDATION

In order to validate the numerical method, a plain rectangular duct was first simulated to compare to literature values. The results show that the fully developed Nusselt numbers converge to the analytic solution (Haji-Sheikh *et al.*, 1983) with a relative error of 1.7% for both the low and high Reynolds number cases. The pressure drop values are comparable to the theoretical pressure drop (Kakaç *et al.*, 1987) with a relative error of 3% for low Reynolds number (3.35Pa) and 3.9% for the high Reynolds number case (25.91 Pa).

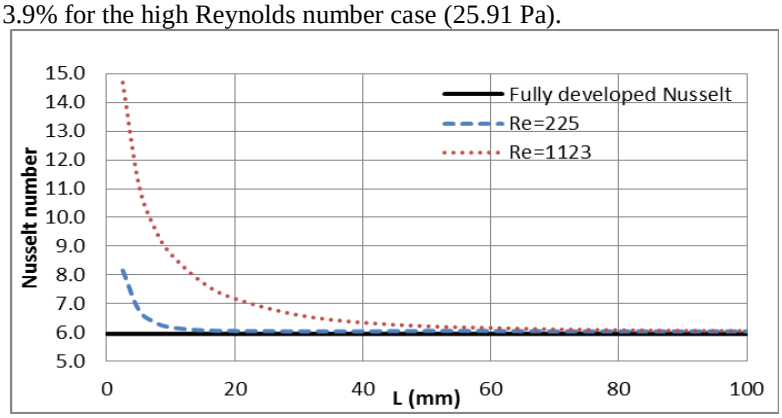

Figure 4: Verification with analytic solution for a plain rectangular channel

A grid independence test was conducted with three different mesh sizes – a coarse mesh with 20x40 (400,000 cells), an intermediate mesh with 40x80 (818,160 cells) and a fine mesh with 80x80 cells (3.1 million cells). The results for fully developed Nusselt number and pressure drop for the intermediate and fine grid are within 0.1% and so the intermediate mesh is considered grid independent for the purpose of this study.

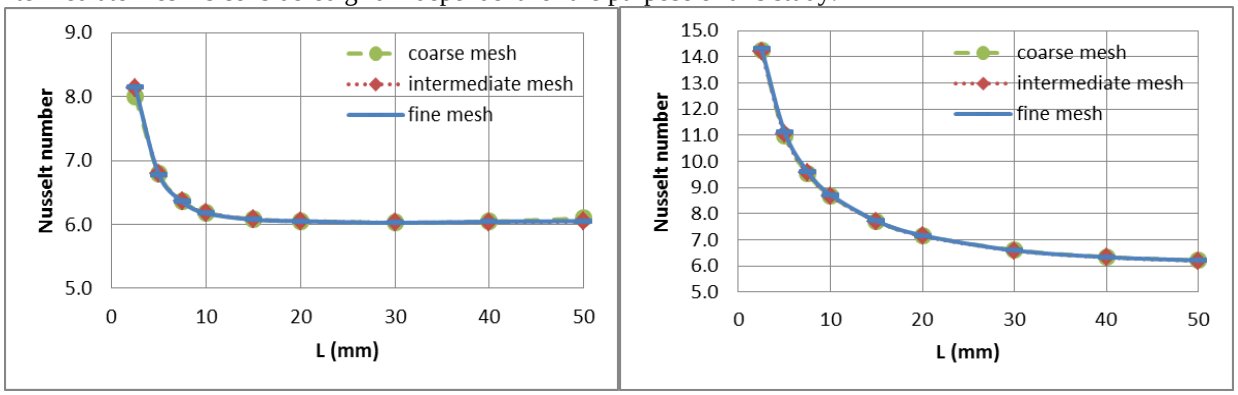

Figure 5: Grid Independence results for low and high Re

The results of the mass transfer experiments give an average Nusselt number which is compared with the numerical simulation. A range of Reynolds numbers from 710 to 1930 is used as permissible by the experimental set up. The geometry and conditions of the experiment are mimicked in the numerical set up. A uniform wall temperature is imposed only on the area where naphthalene is cast and the rest of the wall is adiabatic. An area averaged Nusselt number is obtained from the numerical simulation. The results are within the experimental uncertainty (5.6%) for the first two Reynolds numbers and a difference of 9.6% is seen for the highest Reynolds number case.

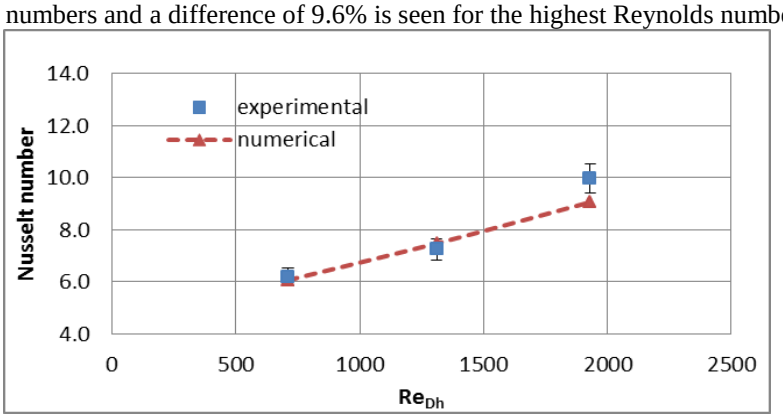

Figure 6: Validation with experiments

5. NUMERICAL RESULTS

Based on the geometry guided by the flow visualization experiments, a VG array consisting of up to three pairs of delta winglets are simulated. The results of the Nusselt number enhancement and the associated pressure drop penalty will be compared to the baseline case for different number of VG pairs and Reynolds numbers. The results for low Re (225) indicate that the ratio of Nusselt number increase to the pressure drop penalty is the highest for one VG pair (1.71) and decreases for two pair (1.54) and three pairs (1.34) of VGs. When the Reynolds number is increased to 1123, there is a good enhancement in Nusselt number of 31.5% associated with a higher pressure drop increase of 45%.

Table 1: Increase in Nusselt number and pressure drop for VG array

Re	No. of VG pairs	ΔP increase	Nu increase
225	1	6.3%	10.8%
	2	12.4%	19.1%
	3	18.3%	24.5%
1123	3	45.0%	31.5%

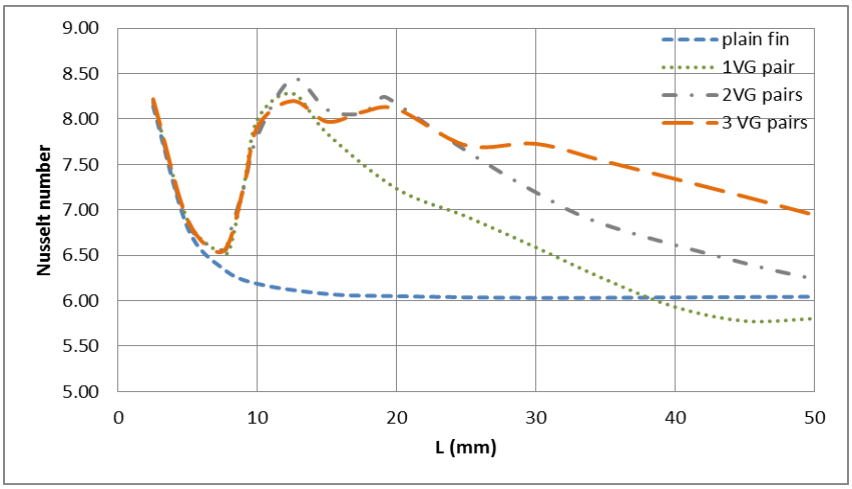

Figure 7: Perimeter-averaged Nusselt numbers along the flow direction

In order to look into why the pressure drop increases significantly, the interaction between vortices is studied by plotting contours of z-vorticity and a comparison is made between the two Reynolds numbers. Figure 8 depicts different cross sections along the flow (z-direction) to study vortex strength normal to the plane. The left side of each figure is a line of symmetry (y=0) and the top, bottom and right sides represent walls. In the low Re case, the vortices dissipate faster and there is not a lot of interaction between the first vortex that is generated with the subsequent vortices. In the high Re case, the vortices generated are stronger and persist through the length of the duct. There are a lot more interactions and a secondary vortex is also generated next to the symmetry line. However the interactions between vortices do not seem to add to the vortex strength but introduces a lot of mixing in the flow. The VGs are located starting at 7.5mm, 16mm and 24.5mm in the z-direction or flow direction.

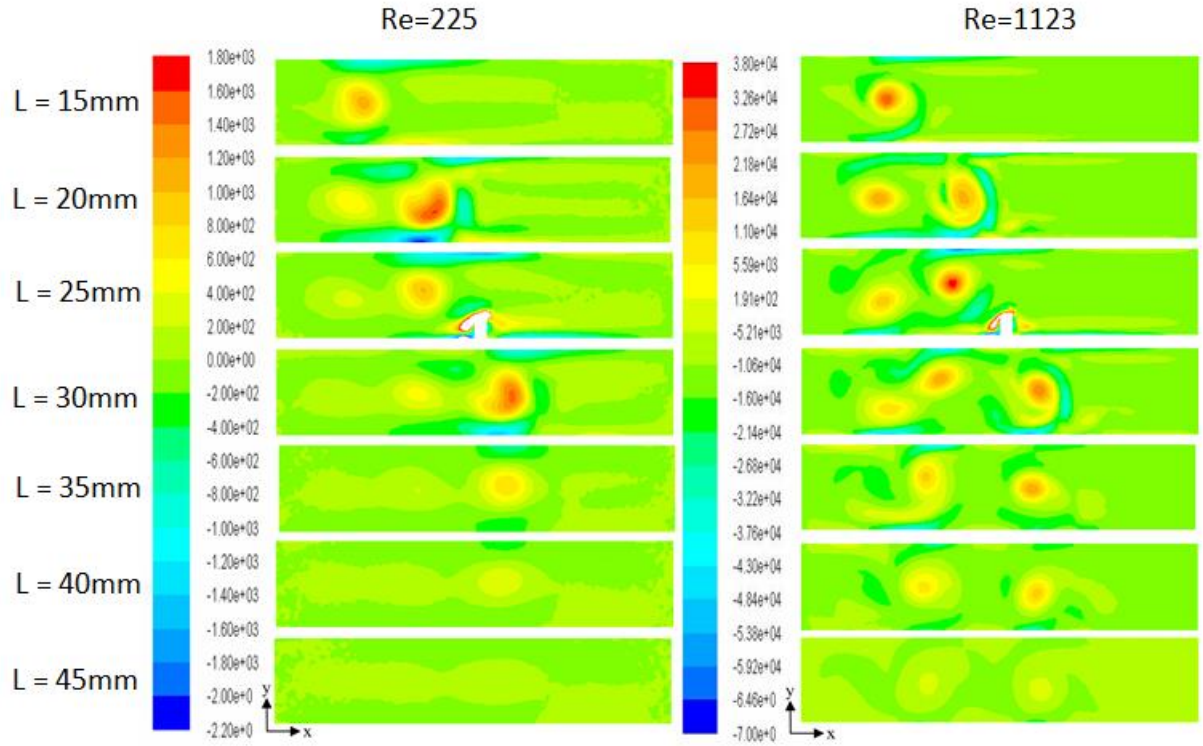

Figure 8: Contours of z- vorticity along the flow direction

On the other hand, VG pairs were placed beside each other on the x-y plane far enough where there is no interaction between the vortices where the heat transfer increased significantly and pressure drop penalty was not much higher than the two VG pair array for low Reynolds number case. The array configuration with two VG pairs has a slightly lower pressure drop when the vortices interact slightly but are able to flow through the channel smoothly. In the high Re case, the Nusselt number increase and pressure drop penalty are almost equal. Based on the Reynolds number the vortex strength increases so the same delta winglets produce stronger vortices that are unable to flow as easily through the channel.

Table 2: VG pairs with no vortex interaction

Re	No. of VG pairs	ΔP increase	Nu increase
225	2	14.1%	23.8%
1123	2	38.2%	38.3%

6. CONCLUSIONS

A numerical study of two different configurations of delta winglet VG in a rectangular channel is carried out at two Reynolds numbers. The heat transfer and pressure drop changes are reported with and without interaction between the generated vortices. The main findings are summarized below:

- Placing delta winglets in the array configuration led to an increase in Nusselt numbers higher than the pressure drop penalty at low Reynolds number.
- Pressure drop is slightly lower for the array in comparison to the straight line formation for two VG pairs, however the increase in Nusselt number is higher in the straight line configuration.
- When no interaction between vortices occurs, there is better performance which suggests that the array may have caused some destructive interference between vortices.
- An optimal VG array may be possible for a fixed Reynolds number so that the behavior of the vortices and interactions can be predicted better to augment vortex strength.

NOMENCLATURE

A_n	area of naphthalene case	(m^2)
B	width of the channel	(mm)
c_p	specific heat of air	(J/kg-K)
$D_{n,a}$	naphthalene diffusion coefficient	(m^2/s)
D_h	hydraulic diameter of channel	(mm)
h_m	average mass transfer coefficient	(m/s)
h	heat transfer coefficient	(W/m^2-K)
H	height of the channel (fin spacing)	(mm)
k	thermal conductivity of air	(W/m^2-K)
L	length of the channel	(mm)
m	mass of naphthalene cast	(kg)
Nu	Nusselt number	
P	Pressure	(Pa)
ΔP	air side pressure drop across the channel length	(Pa)
Pr	Prandtl number	
q	total heat flux	(W/m^2)
Re	Reynolds number based on hydraulic diameter of channel	
Sc	Schmidt number	
Sh	Sherwood number	
t	time	(s)
T	temperature	(K)
T_m	mass averaged temperature	(K)
T_w	wall temperature	(K)
u_i	velocity in x, y and z direction- u, v and w	(m/s)
x_i	direction- x, y and z	
α	thermal diffusivity	(m^2/s)
ρ	density of fluid	(kg/m^3)
$\rho_{n,v}$	naphthalene vapor density	
μ	dynamic viscosity of air	(kg/m-s)
ν	kinematic viscosity of air	(m^2/s)

Subscript

i	index
j	direction vector
w	wall of channel
∞	based on freestream

REFERENCES

Dezan, D. J., Salviano, L. O., & Yanagihara, J. I. (2015). Interaction effects between parameters in a flat-tube louvered fin compact heat exchanger with delta-winglets vortex generators. *Applied Thermal Engineering*, *91*, 1092-1105.

ElSherbini, A. I., & Jacobi, A. M. (2002). The thermal-hydraulic impact of delta-wing vortex generators on the performance of a plain-fin-and-tube heat exchanger. *HVAC&R Research*, *8*(4), 357-370.

Fiebig, M., Valencia, A., & Mitra, N. K. (1993). Wing-type vortex generators for fin-and-tube heat exchangers. *Experimental Thermal and Fluid Science*,*7*(4), 287-295.

Fiebig, M., Valencia, A., & Mitra, N. K. (1994). Local heat transfer and flow losses in fin-and-tube heat exchangers with vortex generators: a comparison of round and flat tubes. *Experimental Thermal and Fluid Science*, *8*(1), 35-45.

Haji-Sheikh, A., Mashena, M., & Haji-Sheikh, M. J. (1983). Heat transfer coefficient in ducts with constant wall temperature. *Journal of heat transfer*,*105*(4), 878-883.

He, Y. L., Chu, P., Tao, W. Q., Zhang, Y. W., & Xie, T. (2013). Analysis of heat transfer and pressure drop for fin-and-tube heat exchangers with rectangular winglet-type vortex generators. *Applied Thermal Engineering*,*61*(2), 770-783.

Joardar, A., & Jacobi, A. M. (2005). Impact of leading edge delta-wing vortex generators on the thermal performance of a flat tube, louvered-fin compact heat exchanger. *International Journal of Heat and Mass Transfer*, *48*(8), 1480-1493.

Joardar, A., & Jacobi, A. M. (2007). A numerical study of flow and heat transfer enhancement using an array of delta-winglet vortex generators in a fin-and-tube heat exchanger. *Journal of Heat Transfer*, *129*(9), 1156-1167.

Joardar, A., & Jacobi, A. M. (2008). Heat transfer enhancement by winglet-type vortex generator arrays in compact plain-fin-and-tube heat exchangers.*International Journal of refrigeration*, *31*(1), 87-97.

Kakaç, S., Shah, R. K., & Aung, W. (Eds.). (1987). *Handbook of single-phase convective heat transfer* (pp. 7-1). New York et al.: Wiley.

Leu, J. S., Wu, Y. H., & Jang, J. Y. (2004). Heat transfer and fluid flow analysis in plate-fin and tube heat exchangers with a pair of block shape vortex generators. *International Journal of Heat and Mass Transfer*, *47*(19), 4327-4338.

Mendes, P. S. (1991). The naphthalene sublimation technique. *Experimental Thermal and Fluid Science*, *4*(5), 510-523.

Tian, L. T., He, Y. L., Lei, Y. G., & Tao, W. Q. (2009). Numerical study of fluid flow and heat transfer in a flat-plate channel with longitudinal vortex generators by applying field synergy principle analysis. *International Communications in Heat and Mass Transfer*, *36*(2), 111-120.

Wang, L. B., Ke, F., Gao, S. D., & Mei, Y. G. (2002). Local and average characteristics of heat/mass transfer over flat tube bank fin with four vortex generators per tube. *Journal of heat transfer*, *124*(3), 546-552.

Wu, J. M., & Tao, W. Q. (2008a). Numerical study on laminar convection heat transfer in a rectangular channel with longitudinal vortex generator. Part A: Verification of field synergy principle. *International Journal of Heat and Mass Transfer*, *51*(5), 1179-1191.

Wu, J. M., & Tao, W. Q. (2008b). Numerical study on laminar convection heat transfer in a rectangular channel with longitudinal vortex generator. Part A: Verification of field synergy principle. *International Journal of Heat and Mass Transfer*, *51*(5), 1179-1191.

ACKNOWLEDGEMENT

This material is based upon work supported by the National Science Foundation under Grant No. CBET 13-57992. The authors would like to acknowledge and thank the Electric Power Research Institute for sponsoring this work especially Dr. Jessica Shi in regards to her technical contribution to the project.